Application and discussion on entransy analysis of ammonia/salt absorption heat pump systems

Lei Yang[1,2,3,4], Sihao Huang[1,2,3,4], Zhenneng Lu[1,2,3], Yulie Gong[1,2,3] and Huashan Li[1,2,3,*]

[1]*Guangzhou Institute of Energy Conversion, Chinese Academy of Sciences, Guangzhou 510640, China;* [2]*CAS Key Laboratory of Renewable Energy, Guangzhou 510640, China;* [3]*Guangdong Provincial Key Laboratory of New and Renewable Energy Research and Development, Guangzhou 510640, China.;* [4]*University of Chinese Academy of Sciences, Beijing 100049, China.*

Abstract

This study investigates the application of the entransy analysis in ammonia/salt absorption heat pump (AHP) systems. The results of the entransy analysis are compared with those of energy analysis and exergy analysis under typical and various operating conditions. Entransy dissipation and exergy loss in each component, as well as coefficient of performance (COP), exergy efficiency and entransy efficiency of systems, are discussed. The changing trends of entransy dissipation in each component are similar under various operating conditions. However, the entransy analysis performs better than the exergy analysis in evaluating the irreversible loss of each component. Moreover, the differences between the exergy analysis and entransy analysis are mainly in absorber, generator and SHE. Especially in the NH_3/NaSCN system, the proportion of entransy dissipation in generator is 60.8%, which is almost twice of the proportion of exergy loss (34.9%). In addition, under various operating conditions, entransy efficiency and COP have roughly the same changing trend. Meanwhile, entransy efficiency is more reasonable than exergy efficiency in evaluating the performance of systems under the absorption temperature, which varies from 30°C to 50°C. These comparison results demonstrate that the entransy analysis is appropriate to evaluate the performance of ammonia/salt AHP systems and suitable for analyzing the irreversibility of each component.

Keywords: entransy; exergy; absorption heat pump; ammonia/salt; performance analysis

*Corresponding author: lihs@ms.giec.ac.cn

Received 17 December 2020; revised 28 February 2021; editorial decision 11 March 2021; accepted 11 March 2021

1. INTRODUCTION

In recent years, absorption heat pump (AHP) has gained great interest. Compared with the conventional vapor compression heat pumps, the AHPs consume less electricity power and can utilize low-grade thermal energy from geothermal, solar and biomass energy sources [1, 2]. In addition, AHP has the advantage of better-friendly economy and environment [3].

The H_2O/LiBr and NH_3/H_2O are the most common used solutions in AHPs; however, some drawbacks of the solutions limit the application of absorption systems [4–6]. For example, the crystallization possibility and high freezing point of the H_2O/LiBr solution, as well as the complex and costly rectifier of the NH_3/H_2O system. Besides, $NH_3/LiNO_3$ and NH_3/NaSCN are considered as substitutes for NH_3/H_2O [7, 8]. Compared to NH_3/H_2O absorption system, $NH_3/LiNO_3$ and NH_3/NaSCN absorption systems avoid rectification equipment and have relatively high coefficient of performance (COP) [9].

Many efforts have been devoted to investigate on the $NH_3/LiNO_3$ and NH_3/NaSCN absorption systems using the energy analysis and exergy analysis. Sun [9] performed the energy analysis for NH_3/H_2O, $NH_3/LiNO_3$ and NH_3/NaSCN single-effect absorption systems and concluded that NH_3/salt systems perform better than the NH_3/H_2O system. Zhu and Gu [10, 11] carried out the energy analysis and exergy analysis on the NH_3/NaSCN absorption system. Farshi *et al.* [7] presented the energy analysis

International Journal of Low-Carbon Technologies 2021, 16, 977–986

https://doi.org/10.1093/ijlct/ctab027 Advance Access publication 3 April 2021

and exergy analysis of $NH_3/LiNO_3$ and NH_3/NaSCN absorption systems, concluding that the possibility of crystallization will be increased by higher generation temperatures. Cai *et al.* [12, 13] improved the exergy analysis method for the $NH_3/LiNO_3$ and NH_3/NaSCN absorption refrigeration systems. Pandya *et al.* [14] evaluated the thermodynamic performance and optimal parameters of ammonia/salt absorption cooling system.

However, the exergy analysis is used to analyze the irreversibility of AHP system from the perspective of heat-work conversion [15]. In the AHP system, the central irreversible loss is caused by the heat and mass transfer process between the internal working solution and external fluid. The concept of entransy dissipation proposed by Guo *et al.* [16] can represent the irreversibility, which is caused by the heat and mass transfer process. Chen *et al.* [17] confirmed that entransy dissipation is appropriate for measuring the irreversibility of the system in the heat transfer process. Zhang *et al.* [18] carried out the entransy analysis in the optimization of HVAC systems. Moreover, Wang *et al.* [19] used the entransy analysis to propose the optimization design of an absorption temperature transformer. Li [20] introduced the entransy dissipation method into the analysis of the internal heat and mass transfer of the absorber and obtained the approach and guiding principles for optimizing the thermodynamic performance of the absorber. Zhang *et al.* [21] conducted the concept of concentration entransy in the entransy analysis of absorption systems and established entransy dissipation calculation model of the H_2O/LiBr absorption system. Above all, compared to the energy analysis and exergy analysis, the entransy analysis method can accurately identify the irreversibility caused by heat and mass transfer of each component in absorption systems. Thus, the information of the entransy analysis indicates the effective direction to improve the performance of absorption systems.

In reviewing the literature, it can be found that the previous studies on $NH_3/LiNO_3$ and NH_3/NaSCN absorption systems mainly used the methods of the energy analysis and exergy analysis. However, few studies have focused on utilizing the method of the entransy analysis in NH_3/salt AHP systems. Thus, in this study, the entransy analysis is proposed to investigate and evaluate the performance of the NH_3/salt AHP systems under typical and various operating conditions. Moreover, the results of the entransy analysis are compared with those of the energy analysis and exergy analysis. In detail, exergy loss and entransy dissipation of each component, as well as COP, exergy efficiency and entransy efficiency of systems under typical and various operating conditions, are evaluated.

2. MODELING

2.1. System description

Before discussion on the entransy analysis of the NH_3/salt AHP systems, it is important to address detailed information on the components and working pairs of the single-effect AHP system. As given in Figure 1, the single-effect AHP system is mainly consisted by a generator, condenser, evaporator, absorber, solution heat exchange (SHE), refrigerant throttle valve (RTV), pump and solution throttle valves (STV). The generator is driven by the high-temperature heat source, where the NH_3 vapor (state 7) is generated from the weak solution (state 3). The strong solution (state 4) passes the SHE (state 5), gets throttled by the STV (state 6) and then enters the absorber absorbing the NH_3 vapor (state 10) from the evaporator. The weak solution (state 1) is pumped by the pump (state 2) and passes the SHE (state 3) before entering the generator. The NH_3 vapor (state 7) generated in the generator goes through the condenser to be condensed into liquid NH_3 (state 8) and subsequently gets throttled by the RTV (state 9). Then, the refrigerant vaporizes in the evaporator (state 10).

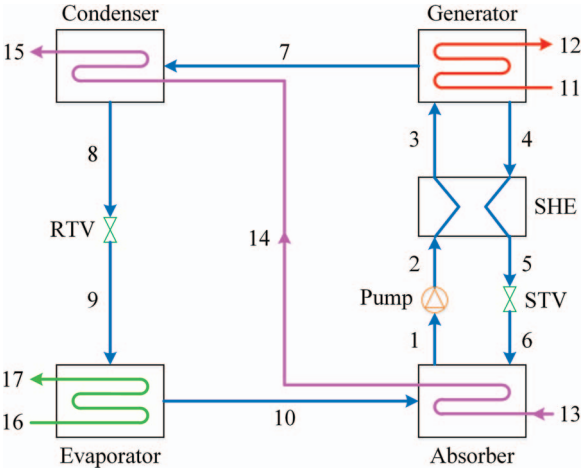

Figure 1. *Schematic diagram of a single-effect AHP system.*

Additionally, as depicted by state 1 to state 6 in Figure 1, the AHP system also includes the solution circle. For the NH_3/salt AHP systems, the solution circle employs two different working pairs, which are $NH_3/LiNO_3$ and NH_3/NaSCN. The thermophysical properties of the two working pairs are obtained from Libotean *et al.* [22, 23], Chaudhari *et al.* [24] and Farshi *et al.* [7, 25]. Meanwhile, in this work, the crystallization concentrations of $NH_3/LiNO_3$ and NH_3/NaSCN in different operating conditions have also been considered. Detailed crystallization concentration equations can be found in Wu *et al.* [6] and Ferreira [26].

2.2. Thermodynamic analysis

In the following section, the equations of the energy analysis, exergy analysis and entransy analysis are applied to the overall components of the system. Moreover, in order to simplify the thermodynamic analysis, some reasonable assumptions are made as follow [27, 28]:

(1) The whole system is operated under steady state conditions.

(2) The heat loss and pressure loss are neglected.

(3) The refrigerants are saturated at the outlet of the condenser and evaporator.

(4) The solutions are under the phase equilibrium condition at the outlet of the generator and absorber.

(5) The throttling process is isenthalpic.

2.2.1. *Energy analysis and exergy analysis*

The energy analysis of the single-effect AHP system is based on the first law of thermodynamics. The basic principles of the first law of thermodynamics are the conservation of mass and energy, as given in equations (1) to (3)

$$\sum m_i - \sum m_o = 0 \tag{1}$$

$$\sum m_i x_i - \sum m_o x_o = 0 \tag{2}$$

$$\sum Q - \sum W = \sum m_o h_o - \sum m_i h_i \tag{3}$$

The COP of the single-effect AHP system is defined as follows:

$$COP = \frac{Q_a + Q_c}{Q_g + W_p} \tag{4}$$

The solution circulation ratio is defined as follows:

$$f = \frac{m_w}{m_0} = \frac{1 - x_s}{x_w - x_s} \tag{5}$$

where the subscripts w and s represent the weak and strong refrigerant solutions, respectively.

The energy analysis detailed above provides quantitative results of the single-effect AHP system. However, the exergy analysis is capable of identifying and quantifying the exergy and exergy loss of components in the single-effect AHP system. Exergy is the maximum theoretical useful work received from energy under the environment. The specific exergy of each stream and the exergy loss of each component are given in equations (6) and (7), respectively.

$$\psi = (h - h_0) - T_0 (s - s_0) \tag{6}$$

The exergy loss of each component can be written as

$$\Delta\psi = \sum m_i \psi_i - \sum m_o \psi_o + Q\left(1 - \frac{T_0}{T}\right) - W \tag{7}$$

The overall exergy loss of the single-effect AHP system is the sum of all components, as given in equation (8):

$$\Delta\psi = \sum \Delta\psi_j = \Delta\psi_a + \Delta\psi_c + \Delta\psi_e + \Delta\psi_g + \Delta\psi_{sh} \tag{8}$$

The efficiency of the second law of thermodynamics for the single-effect AHP system can be evaluated by the exergy efficiency. The exergy efficiency (η_e) indicates the ratio of the output hot water exergy in absorber and condenser to the input driving exergy in generator, which is detailed in equation (9):

$$\eta_e = \frac{m_{13}(\psi_{15} - \psi_{13})}{m_{11}(\psi_{11} - \psi_{12})} \tag{9}$$

2.2.2. *Entransy analysis*

In addition to the energy analysis and exergy analysis, the entransy analysis is also employed to evaluate the performance of absorption systems. Entransy is a physical quantity that represents the heat transfer ability of an object [16].

The entransy dissipation can be expressed as follows:

$$\Delta G = \int_0^{Q_1} \Delta T dQ \tag{10}$$

In absorption system, the entransy dissipation can also be expressed as follows:

$$\Delta G_j = -\left(\Delta G_{w,j} + \Delta G_{v,j} + \Delta G_{s,j} + \Delta G_{x,j}\right) \tag{11}$$

(11)where ΔG_w is the variation in the external water entransy, ΔG_x is the variation in the solution concentration entransy, ΔG_s is the variation in the solution heat entransy and ΔG_v is the variation in the vapor entransy.

It is worth noting that the changes in solution concentration entransy and solution heat entransy are not included in condenser and evaporator. Meanwhile, the solution heat entransy is the only parameter considered in SHE. The entransy dissipation calculation model of the single-effect absorption system can be found in the previous investigation [21].

The overall entransy dissipation of the single-effect AHP system is the sum of all components:

$$\Delta G = \sum \Delta G_j = \Delta G_a + \Delta G_c + \Delta G_e + \Delta G_g + \Delta G_{sh} \tag{12}$$

The entransy efficiency of the single-effect AHP system is defined as follows:

$$\eta_g = \frac{Q_a T_a + Q_c T_c}{Q_g T_g} \tag{13}$$

where T_a, T_c and T_g are the absorption temperature, condensation temperature and generation temperature during system operation, respectively.

2.3. Model validation

For the purpose of verifying the accuracy of the single-effect NH_3/salt AHP model, the simulation results are validated by comparing with the results reported by Farshi *et al.* [7], as shown in Table 1. It can be seen that, under the same operating conditions, the simulation results of the proposed model show good

Table 1. *Comparison between simulation results from Farshi et al. [7] and this work.*

T_g [°C]	$T_a = T_c$ [°C]	T_e [°C]	COP This work	COP Ref. [7]	Deviation
			$NH_3/LiNO_3$ system		
85	35	0	0.5449	0.5414	0.65%
90	35	0	0.5645	0.5606	0.70%
95	35	0	0.5725	0.5694	0.54%
100	35	0	0.5748	0.5715	0.58%
105	35	0	0.5742	0.5715	0.47%
110	35	0	0.5719	0.5685	0.60%
			NH_3/NaSCN system		
85	35	0	0.579	0.5863	-1.25%
90	35	0	0.6168	0.6187	-0.31%
95	35	0	0.6357	0.6329	0.44%
100	35	0	0.6436	0.6370	1.04%
105	35	0	0.6468	0.6388	1.25%
110	35	0	0.6473	0.6364	1.71%

Table 2. *Input parameters for typical operating conditions.*

Parameters	Value
Absorption temperature, T_a [°C]	45
Condensation temperature, T_c [°C]	50
Evaporation temperature, T_e [°C]	10
Generation temperature, T_g [°C]	110
Heating capacity, Q_h [kW]	100
Effectiveness of SHE, η_s [−]	0.7
Pump efficiency, η_p [−]	0.9
Environment pressure, P_0 [kPa]	101.3
Environment temperature, T_0 [°C]	25

agreements with the published results. It is therefore concluded that the present model is reliable and can be used to investigate the performance of the single-effect NH_3/salt AHP systems.

3. RESULTS AND DISCUSSIONS

In this section, the entransy analysis in NH_3/salt AHP systems has been investigated and evaluated under typical and various operating conditions. Meanwhile, the obtained results of entransy analysis have been compared with those of the energy analysis and exergy analysis. Detailed results and discussions are given in Sections 3.1 and 3.2.

3.1. Typical operating conditions

Under typical operating conditions, the operating parameters of the systems are listed in Table 2. The inlet/outlet temperatures of the high-temperature water used in generator are 125/115°C. The returned water from the users flowing through absorber and condenser in series and the low-temperature water used in evaporator are 35/45°C and 17/12°C, respectively. The operating parameters are specified according to the application in floor heating [8].

Table 3. *The simulation results of ammonia/salt AHP systems.*

Working pairs	$NH_3/LiNO_3$	NH_3/NaSCN
x_w [−]	0.51	0.47
x_s [−]	0.42	0.41
Q_a [kW]	57.8	55.5
Q_c [kW]	42.2	44.5
Q_e [kW]	35.2	37.2
Q_g [kW]	64.4	62.2
Q_{sh} [kW]	26.0	28.9
W [kW]	0.4	0.6
f [−]	6.7	9.6
COP [−]	1.544	1.592
$\Delta\psi$ [kW]	9.16	8.59
ΔG [kW·K]	4410.3	4148.7
η_e [−]	0.306	0.317
η_g [−]	1.297	1.343

By employing the parameters listed in Table 1, the simulated results of NH_3/salt AHP systems have been given in Table 3. The concentration difference between the weak and strong solutions demonstrates that the solution circulation ratio of the $NH_3/LiNO_3$ system is lower than that of the NH_3/NaSCN system. However, COP of the NH_3/NaSCN system (1.592) is higher than that of the $NH_3/LiNO_3$ system (1.544). This result can be explained by the fact that exergy loss and entransy dissipation of the NH_3/NaSCN system are lower than those of the $NH_3/LiNO_3$ system. Meanwhile, exergy efficiency and entransy efficiency of the NH_3/NaSCN system are also higher than those of the $NH_3/LiNO_3$ system.

For the purpose of comparing the exergy analysis and entransy analysis under typical operating conditions, the statistic results of exergy loss and entransy dissipation for each component have been shown in Figure 2. The column figure indicates that the generator plays a main role in irreversible losses of NH_3/salt AHP systems, either for exergy loss or entransy dissipation. Meanwhile, the proportions of exergy loss and entransy dissipation in evaporator are the lowest in the overall system, as can be observed from Figure 2. The proportions of exergy loss in absorber and condenser are almost equal to those of the entransy dissipation. The similar results of the $NH_3/LiNO_3$ system and NH_3/NaSCN system further verify the reliability of the entransy analysis in NH_3/salt AHP systems. However, the differences between exergy loss and entransy dissipation can also be found. Specifically, for NH_3/NaSCN system, exergy loss in SHE is as large as 29.7%, while entransy dissipation is only 15.8%. Although the proportions of exergy loss and entransy dissipation in generator are the largest, the dramatic distinctions between the values of exergy loss and entransy dissipation still exist. In the NH_3/NaSCN system, the proportion of entransy dissipation (60.8%) in the generator is almost twice that of exergy loss (34.9%).

The entransy dissipation analysis can distinguish the irreversible losses caused by heat and mass transfer in each component of absorption systems. Table 4 lists the specific irreversible losses in each component of NH_3/salt AHP systems using entransy dissipation analysis. As can be seen in Table 4, the

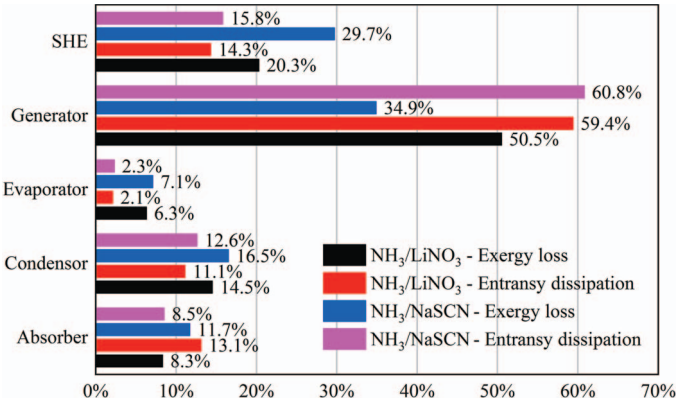

Figure 2. *Exergy loss and entransy dissipation in each component.*

Table 4. *Entransy dissipation [kW·K] of each component in ammonia/salt AHP systems.*

Components	ΔG_w	ΔG_v	ΔG_s	ΔG_x	Entransy dissipation
$NH_3/LiNO_3$ system					
Absorber	2190.2	-418.5	-412.9	-1937.3	578.5
Condenser	1809.8	-2299.7			489.9
Evaporator	-510.6	418.5			92.1
Generator	-7731.3	2675.9	686.1	1750.6	2618.7
SHX			-631.0		631.0
Total					4410.2
NH_3/NaSCN system					
Absorber	2094.7	-441.8	-131.0	-1874.1	352.2
Condenser	1905.4	-2427.8			522.4
Evaporator	-539.1	441.8			97.3
Generator	-7469.6	2824.9	176.3	1946.4	2522.0
SHX			-654.8		654.8
Total					4148.7

variations in the external water entransy and solution concentration entransy are greatly in absorber. In generator, the variation of external water entransy is the greatest (−7731.3 kW·K for $NH_3/LiNO_3$ system, −7469.6 kW·K for NH_3/NaSCN system) due to the large temperature difference between the inlet and outlet of driving hot water. Moreover, entransy dissipation in SHE is large than that in absorber and condenser. In general, larger entransy dissipation means larger irreversible loss. Reducing entransy dissipation of component can improve its performance. Therefore, the information from the entransy dissipation analysis indicates the most effective direction to improve performance of absorption systems. Additionally, it can be seen that the significant difference between the $NH_3/LiNO_3$ system and NH_3/NaSCN system is the variation in the solution heat entransy of absorber (−412.9 kW·K for $NH_3/LiNO_3$ system, −131.0 kW·K for NH_3/NaSCN system). It can be therefore concluded that, under typical operating conditions, the entransy analysis is appropriate in the NH_3/salt AHP systems. The entransy dissipation method performs better than the exergy loss method in investigating and evaluating the irreversible loss of each component in absorption systems.

3.2. Various operating conditions

For the purpose of further evaluating the performance of entransy analysis method in NH_3/salt AHP systems, it is critical to investigate the entransy dissipation in each component and entransy efficiency of systems under various operating conditions. Therefore, the changes in generation temperature (T_g), absorption (T_a) and condensation ($T_c = T_a + 5$) temperatures, as well as evaporation temperature (T_e), are considered. The comparison results among COP, exergy efficiency and entransy efficiency of systems are discussed in this section.

3.2.1. *Generation temperature*

In order to investigate the performance of the entransy analysis method in NH_3/salt AHP systems under different generation temperature conditions, the exergy loss analysis and entransy dissipation analysis of NH_3/salt AHP systems are given in Figures 3 and 4, respectively. As shown in Figure 3, the total exergy loss and total entransy dissipation in $NH_3/LiNO_3$ system increase with the increasing of generation temperature. Moreover, the changing trends of exergy loss and entransy dissipation in each component are similar. Specifically, as the generation temperature increases, the growth of exergy loss and entransy dissipation in generator and absorber are faster than those in condenser. The exergy loss and entransy dissipation in evaporator remain almost consistent. However, there are some discrepancies between the values of exergy loss and entransy dissipation in SHE, as can be seen from Figure 3a and b. The exergy loss in SHE in Figure 3a is always higher than that in absorber, but the entransy dissipation in SHE in Figure 3b is gradually lower than that in absorber. Figure 4 shows the exergy loss and entransy dissipation in the NH_3/NaSCN system under various generation temperature conditions. Similarly, the total exergy loss and total entransy dissipation in the NH_3/NaSCN system keep rising with the increasing of generation temperature. The changing trends of exergy loss and entransy dissipation in each component are similar. However, the exergy loss in SHE in Figure 4a is larger than that in generator under low generation temperature conditions. The entransy dissipation in SHE in Figure 4b is much lower than that in generator under various generation temperature conditions.

The simulation results from Figures 3 and 4 demonstrate that the variations of entransy dissipation and exergy loss in NH_3/salt AHP systems have the same trend under various generation temperature conditions. However, the values of entransy dissipation and exergy loss have some discrepancies in analyzing the irreversible losses in SHE, especially in the NH_3/NaSCN system. These results may be related to the selection of the reference state in the exergy loss analysis, which leading to excessive exergy loss in SHX. The entransy dissipation is not related to the reference state and is proportional to local temperature difference [21]. Above all, the entransy analysis based on the transport phenomena is suitable for analyzing the irreversibility of each component in NH_3/salt AHP systems under various generation temperature conditions.

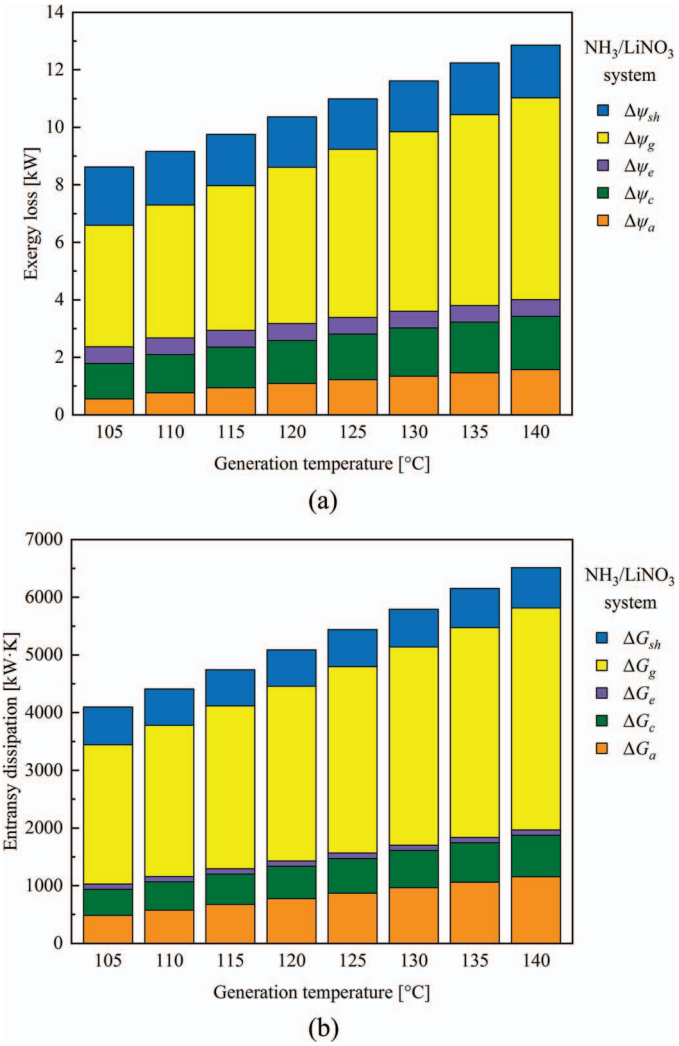

Figure 3. *Variations of (a) exergy loss and (b) entransy dissipation with the increase of generation temperature in the $NH_3/LiNO_3$ system.*

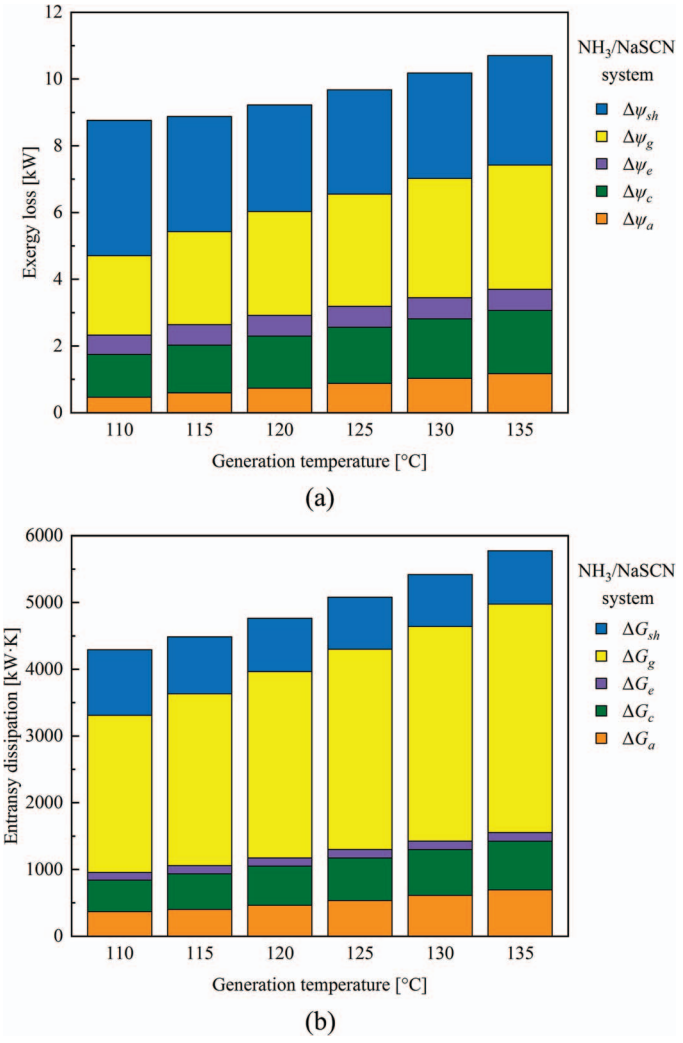

Figure 4. *Variations of (a) exergy loss and (b) entransy dissipation with the increase of generation temperature in the $NH_3/NaSCN$ system.*

Another aspect, COP, exergy efficiency and entransy efficiency are the key factors in analyzing the performance of NH_3/salt AHP systems. As can be seen in Figure 5, with the increasing of generation temperature, COP, exergy efficiency and entransy efficiency of both systems increase first and then decrease. Specifically, entransy efficiency and exergy efficiency have the same changing trend. After reaching their maximum values, entransy efficiency and exergy efficiency continue to decrease. However, the value of COP slightly decreases after reaching the maximum. The results can be explained by the fact that the higher generation temperature causes the generator to produce more NH_3 vapor, which increases the concentration difference between the weak and strong solutions and improves the performance of system. This contributes positively to COP, exergy efficiency and entransy efficiency. However, a too high generation temperature may lead to more irreversible losses (shown in Figures 3 and 4), which has a negative impact on COP, exergy efficiency and entransy efficiency. Moreover, the values of COP, exergy efficiency and entransy efficiency reach the maximum when the generation temperature are 117°C, 96°C and 102°C for the $NH_3/LiNO_3$ system and 126°C, 100°C and 108°C for the NH_3/NaSCN system.

It is evident that COP, exergy efficiency and entransy efficiency of the $NH_3/LiNO_3$ system are higher than those of the NH_3/NaSCN system under the generation temperatures lower than 100°C. Moreover, the possibility of crystallization is also an important problem for NH_3/salt AHP systems. The mark of 'X' indicates that crystallization may occur here. In general, the crystallization of the working solution is most likely to occur at the entrance of the absorber [6, 7]. It can be seen that solution crystallization in the NH_3/NaSCN system is likely to take place under the generation temperature higher than 136°C, as shown in Figure 5. The $NH_3/LiNO_3$ system will not crystallize under various generation temperature conditions.

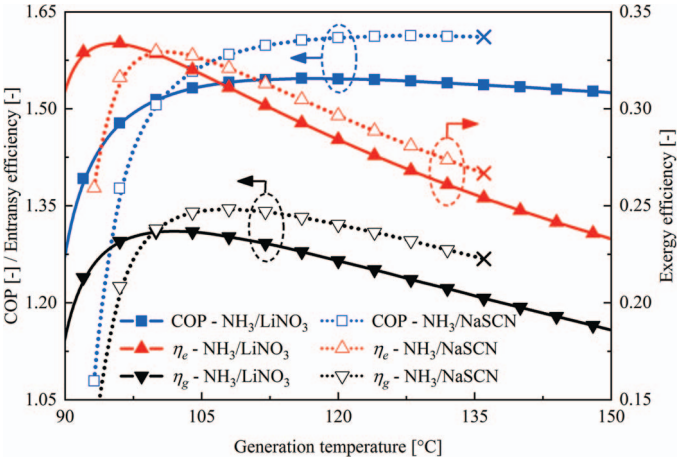

Figure 5. *Variation of COP, exergy efficiency and entransy efficiency with the generation temperature.*

3.2.2. *Absorption and condensation temperatures*

The exergy loss analysis and entransy dissipation analysis of NH_3/salt AHP systems under various absorption (T_a) and condensation ($T_c = T_a + 5$) temperature conditions are given in Figures 6 and 7, respectively. Figure 6 shows that the total exergy loss and total entransy dissipation in $NH_3/LiNO_3$ system decrease with the increasing of absorption and condensation temperatures. In addition, the changing trends of exergy loss and entransy dissipation in each component are similar. With the absorption temperature increases from 32°C to 46°C, the exergy loss and entransy dissipation in absorber, condenser and evaporator show a downward trend. Exergy loss in generator decreases by 31.3%, while entransy dissipation in generator drops by 16.4%. Exergy loss in SHE increases by 41.4% and entransy dissipation in SHE rises by 51.7%. As shown in Figure 7, the total exergy loss and total entransy dissipation in the NH_3/NaSCN system decrease with the increasing of absorption and condensation temperatures. The changing trends of exergy loss and entransy dissipation in each component of NH_3/NaSCN system and $NH_3/LiNO_3$ system are similar. However, exergy loss in SHE in Figure 7a is larger than that in generator under high absorption and condensation temperature conditions. Entransy dissipation in SHE in Figure 7b is much lower than that in generator under various absorption and condensation temperature conditions. Those comparison results in Figures 6 and 7 indicate that the total entransy dissipation of NH_3/salt AHP systems decrease with the increasing of absorption and condensation temperatures. There are some differences between the values of exergy loss and entransy dissipation in generator and SHE under various absorption and condensation temperature conditions, especially in the NH_3/NaSCN system.

Figure 8 shows the variations of COP, exergy efficiency and entransy efficiency with the absorption and condensation temperatures of NH_3/salt AHP systems. The simulation results reveal that, with the increasing of absorption and condensation temperatures, COP continues to decrease, while exergy efficiency keeps growing. Meanwhile, entransy efficiency slightly increases first

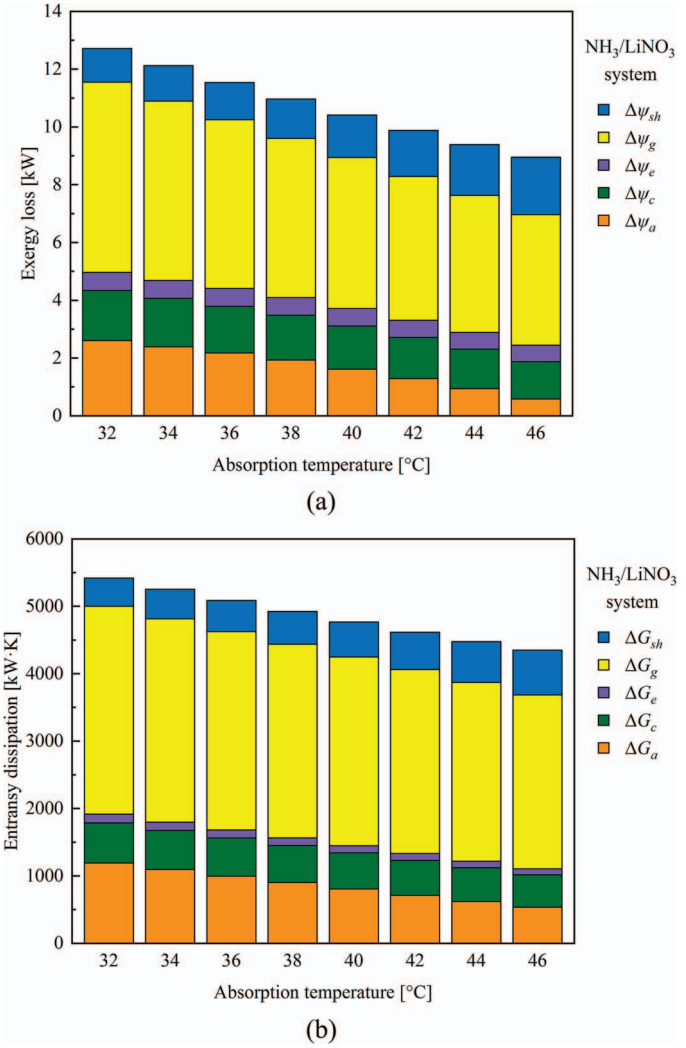

Figure 6. *Variations of (a) exergy loss and (b) entransy dissipation with the increase of absorption and condensation temperatures in the $NH_3/LiNO_3$ system.*

and then decrease with the increase of these temperatures. But actually, excessive absorption and condensation temperatures will reduce the performance of absorption systems. As the absorption and condensation temperatures increase, the absorption and condensation pressures become higher, resulting in the deterioration of the separation process in generator and absorption processes in absorber. Under various absorption and condensation temperature conditions, the changing trends of COP, exergy efficiency and entransy efficiency based on different analysis methods have some differences. In addition, the simulation results from Figure 8 also demonstrate that COP and entransy of NH_3/NaSCN system are higher than those of the $NH_3/LiNO_3$ system when the absorption temperature below 48°C. At the same time, exergy efficiency of NH_3/NaSCN system is slightly higher than that of the $NH_3/LiNO_3$ system. These comparison results in Figure 8 manifest that entransy efficiency is more reasonable than exergy

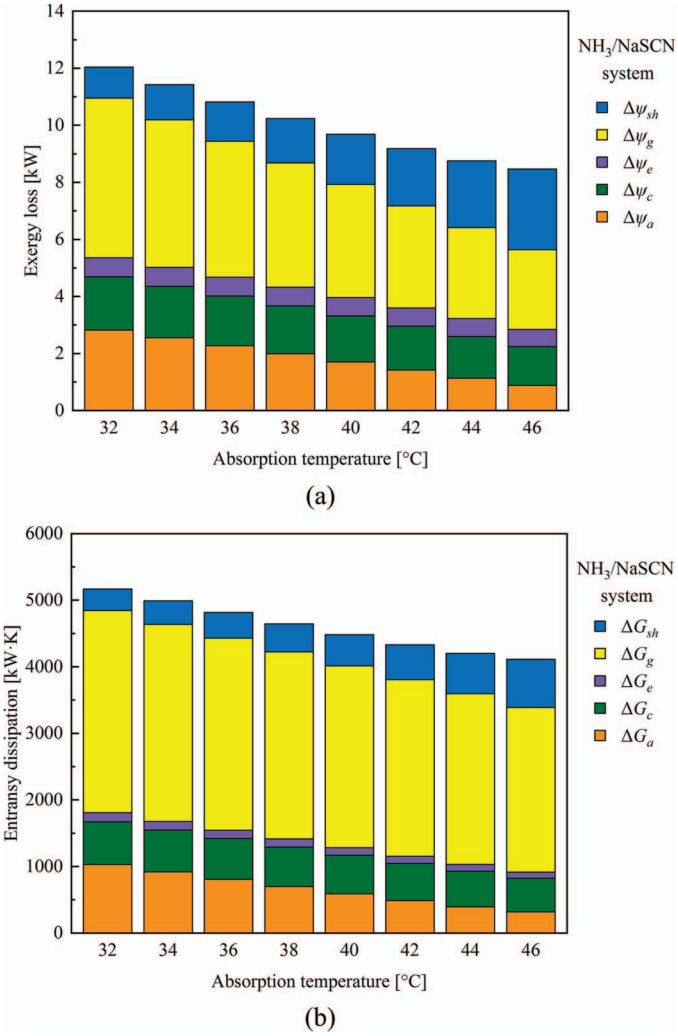

Figure 7. *Variations of (a) exergy loss and (b) entransy dissipation with the increase of absorption and condensation temperatures in the NH_3/NaSCN system.*

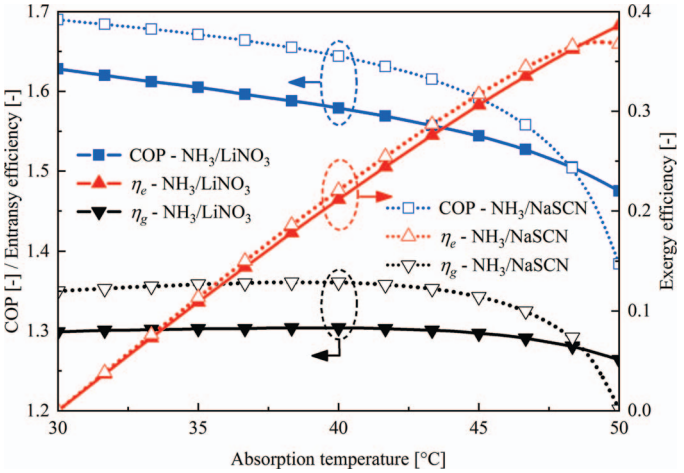

Figure 8. *Variation of COP, exergy efficiency and entransy efficiency with the absorption and condensation temperatures.*

efficiency in analyzing the performance of NH_3/salt AHP systems under various absorption and condensation temperature conditions.

3.2.3. *Evaporation temperature*

The exergy loss analysis and entransy dissipation analysis of NH_3/salt AHP systems under various evaporation temperature conditions are shown in Figures 9 and 10, respectively. The simulation results of $NH_3/LiNO_3$ system in Figure 9 show the total exergy loss increases from 8.65 kW to 9.39 kW and the total entransy dissipation slightly decreases first and then increases with the evaporation temperature increases from 6°C to 20°C. Additionally, in Figure 9a, the exergy loss in absorber rises rapidly by 1772.3%. The exergy loss in SHE decreases dramatically by 57.8%. The exergy losses in condenser and generator increase by 12.7% and 5.6%, respectively. In Figure 9b, the entransy dissipation in absorber only increases by 16.5%. Entransy dissipation in SHE decreases by 44.0%. Entransy dissipation in condenser and generator increases by 12.5% and 11.9%, respectively. Furthermore, as shown in Figure 10, the differences between exergy loss and entransy dissipation in NH_3/NaSCN system can also be found. Specifically, in Figure 10a, exergy loss in generator rises sharply by 55.7%. Exergy loss in SHE is larger than that in generator under low evaporation temperature conditions. In Figure 10b, entransy dissipation in generator only increases by 16.3%, while entransy dissipation in SHE is much lower than that in generator. Moreover, in absorber, with the evaporation temperature increases from 6°C to 20°C, exergy loss increases dramatically by 236%, while the entransy dissipation only rises by 25.7%. Above all, we can draw the conclusion that the total entransy dissipation of NH_3/salt AHP systems decrease with the increasing of evaporation temperature. The changing trends of exergy loss and entransy dissipation in absorber are quite different under various evaporation temperature conditions. Additionally, there are some differences between the values of exergy loss and entransy dissipation in generator and SHE of NH_3/salt AHP systems.

The variations of COP, exergy efficiency and entransy efficiency with the evaporation temperature of NH_3/salt AHP systems are given in Figure 11. It can be seen that, with the increase of evaporation temperature, the values of COP, exergy efficiency and entransy efficiency have a tendency to grow slowly. As the evaporation temperature increases, the evaporation pressure becomes higher. Therefore, the absorption process is strengthened, and the solution concentration difference is enlarged. The circulation ratio becomes smaller, which helps to improve performance of absorption systems. In addition, the values of three indicators of the NH_3/NaSCN system are greater than those of the $NH_3/LiNO_3$ system under various evaporation temperature conditions. Hence, it is noted that from the comparison results the entransy efficiency is suitable for investigating the performance of NH_3/salt AHP systems under various evaporation temperature conditions.

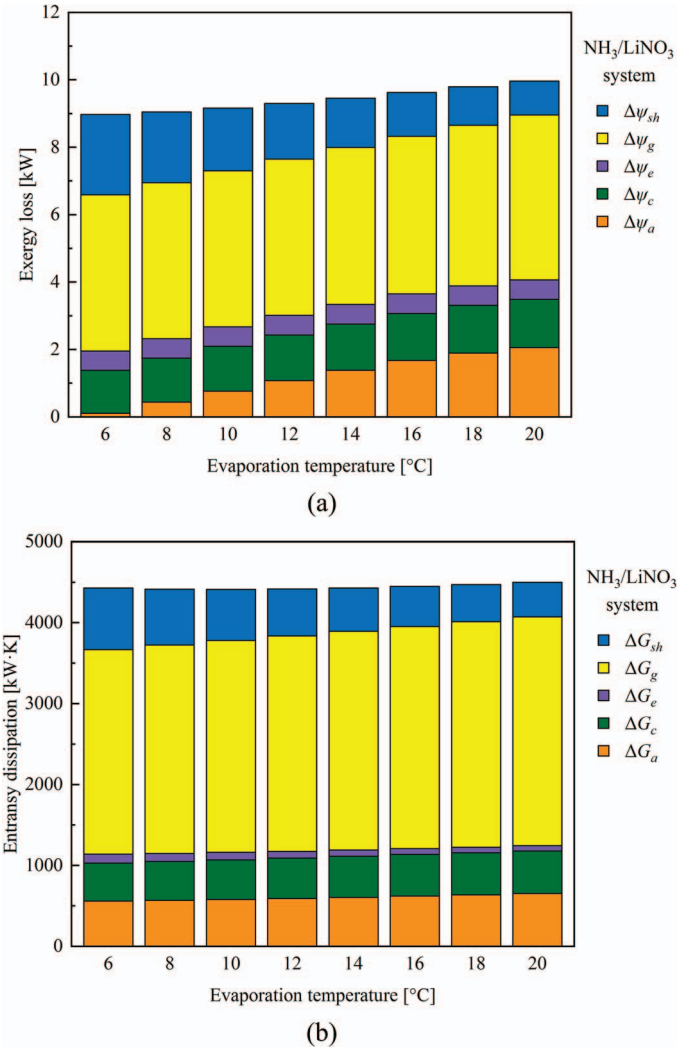

Figure 9. *Variations of (a) exergy loss and (b) entransy dissipation with the increase of evaporation temperature in the $NH_3/LiNO_3$ system.*

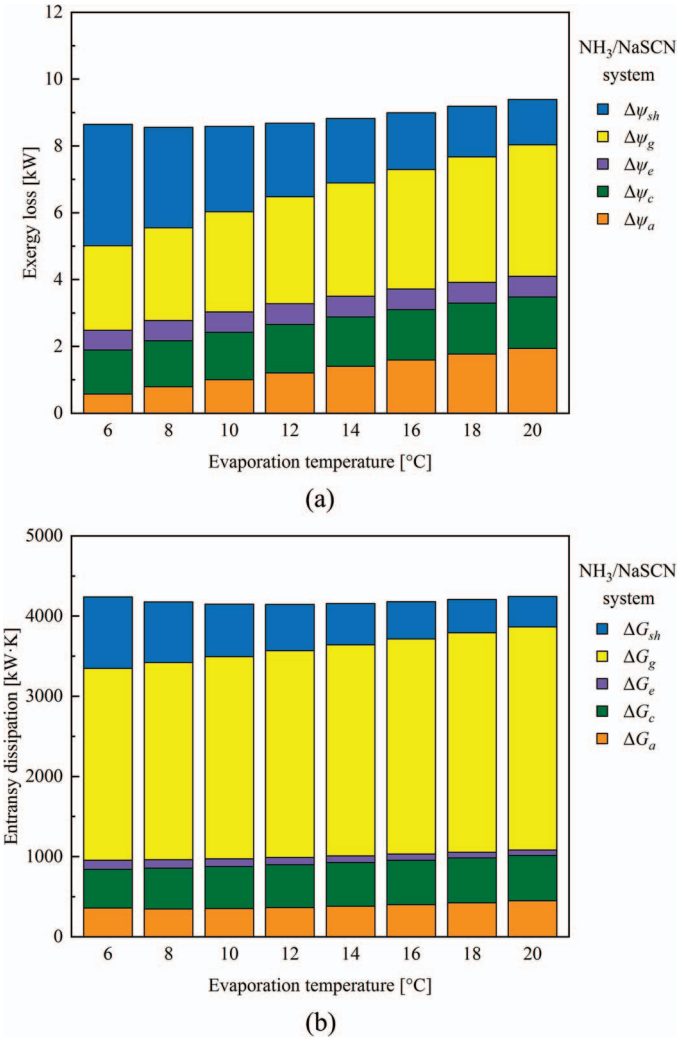

Figure 10. *Variations of (a) exergy loss and (b) entransy dissipation with the increase of evaporation temperature in the $NH_3/NaSCN$ system.*

4. CONCLUSIONS

In this study, the application of entransy analysis in NH_3/salt AHP systems under typical and various operating conditions is discussed. Moreover, the results of entransy analysis are compared and verified with those of energy analysis and exergy analysis. The main conclusions can be drawn as follows:

(1) The entransy dissipation method performs better than the exergy loss method in investigating and evaluating the irreversible loss of each component in NH_3/salt AHP systems. The differences between the exergy loss analysis and entransy dissipation analysis are mainly in absorber, generator and SHE. Especially in NH_3/NaSCN system, the proportion of entransy dissipation in generator is 60.8%, while the proportion of exergy loss is only 34.9%. In addition, the changing trends of entransy dissipation in each component of NH_3/NaSCN and $NH_3/LiNO_3$ systems are similar under various operating conditions.

(2) Under various operating conditions, entransy efficiency and COP of NH_3/salt AHP systems have roughly the same changing trend. Moreover, entransy efficiency is more reasonable than exergy efficiency in evaluating the performance of systems under the absorption temperature varies from 30°C to 50°C. Under various evaporation temperature conditions, the value of entransy efficiency of the NH_3/NaSCN system is higher than that of the $NH_3/LiNO_3$ system. Similar results can also be obtained at higher generation temperature, as well as lower absorption and condensation temperatures.

(3) To summarize, the entransy analysis is appropriate to evaluate the performance of NH_3/salt AHP systems and suitable for analyzing the irreversibility of each component in the systems.

Further work should be focused on reducing the irreversible loss of each component and improving the performance of NH_3/salt AHP systems by using the method of entransy analysis.

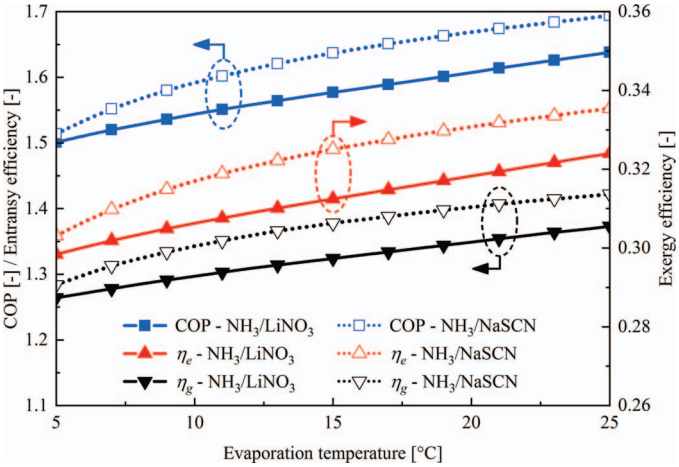

Figure 11. *Variation of COP, exergy efficiency and entransy efficiency with the evaporation temperature.*

ACKNOWLEDGEMENTS

This research is financially supported by the National Key Research and Development Program of China (No. 2019YFB150 4105), Strategic Priority Research Program of Chinese Academy of Sciences (No. XDA21050500), Shandong Major Science and Technology Innovation Projects (No. 2019JZZY010910) and Science and Technology Service Network Initiative Project of Chinese Academy of Sciences (No. KFJ-STS-QYZX-114).

REFERENCES

[1] Valles M, Bourouis M, Boer D. Solar-driven absorption cycle for space heating and cooling. *Appl Therm Eng* 2020;**168**:114836.
[2] Mortazavi M, Schmid M, Moghaddam S. Compact and efficient generator for low grade solar and waste heat driven absorption systems. *Appl Energ* 2017;**198**:173–9.
[3] Wu W, Wang BL, Shi WX *et al.* Absorption heating technologies: a review and perspective. *Appl Energ* 2014;**130**:51–71.
[4] Wang K, Abdelaziz O, Kisari P *et al.* State-of-the-art review on crystallization control technologies for water/LiBr absorption heat pumps. *Int J Refrig* 2011;**34**:1325–37.
[5] Wang YN, Li N, Luo CH. Thermodynamic performance of absorption-compression hybrid refrigeration cycles based on lithium nitrate+1-butyl-3-methylimidazolium nitrate/water working fluid. *Int J Energ Res* 2020;**44**:10394–413.
[6] Wu W, Wang BL, Shi WX *et al.* Crystallization analysis and control of ammonia-based air source absorption heat pump in cold regions. *Adv Mech Eng* 2013;140341:1–10.
[7] Farshi LG, Ferreira CAI, Mahmoudi SMS *et al.* First and second law analysis of ammonia/salt absorption refrigeration systems. *Int J Refrig* 2014;**40**:111–21.
[8] Wu W, Zhang XL, Li XT *et al.* Comparisons of different working pairs and cycles on the performance of absorption heat pump for heating and domestic hot water in cold regions. *Appl Therm Eng* 2012;**48**:349–58.
[9] Sun DW. Comparison of the performances of NH_3-H_2O, NH_3-$LiNO_3$ and NH_3-NaSCN absorption refrigeration systems. *Energ Convers Manage* 1998;**35**:357–68.
[10] Zhu L, Gu J. Thermodynamic analysis of a novel thermal driven refrigeration system. *World Acad Sci Eng Technol* 2009;**56**:351–5.
[11] Zhu L, Gu J. Second law-based thermodynamic analysis of ammonia/-sodium thiocyanate absorption system. *Renew Energ* 2010;**35**:1940–6.
[12] Cai DH, He GG, Tian QQ *et al.* Exergy analysis of a novel air-cooled non-adiabatic absorption refrigeration cycle with NH_3-NaSCN and NH_3-$LiNO_3$ refrigerant solutions. *Energ Convers Manage* 2014;**88**:66–78.
[13] Cai DH, He GG, Tian QQ *et al.* Thermodynamic analysis of a novel air-cooled non-adiabatic absorption refrigeration cycle driven by low grade energy. *Energ Convers Manage* 2014;**86**:537–47.
[14] Pandya B, Modi N, Kumar V *et al.* Performance comparison and optimal parameters evaluation of solar-assisted NH_3-NaSCN and NH_3-$LiNO_3$ type absorption cooling system. *J Therm Anal Calorim* 2019;**135**:3437–52.
[15] Yi YH, Xie XY, Jiang Y. A two-stage vertical absorption heat exchanger for district heating system. *Int J Refrig* 2020;**114**:19–31.
[16] Guo ZY, Zhu HY, Liang XG. Entransy—a physical quantity describing heat transfer ability. *Int J Heat Mass Tran* 2007;**50**:2545–56.
[17] Chen Q, Zhu H, Pan N *et al.* An alternative criterion in heat transfer optimization. *Proc R Soc A* 2011;**467**:1012–28.
[18] Zhang L, Liu X, Jiang Y. Application of entransy in the analysis of HVAC systems in buildings. *Energy* 2013;**53**:332–42.
[19] Wang S, Xie XY, Jiang Y. Optimization design of the large temperature lift/drop multi-stage vertical absorption temperature transformer based on entransy dissipation method. *Energy* 2014;**68**:712–21.
[20] Li JY. Research on heat and mass transfer and match properties of absorber in absorption heat pump. *Ph.D. Thesis*. Tsinghua University, 2016.
[21] Zhang XY, Wu JD, Li Z. Irreversibility characterization and analysis of coupled heat and mass transfer processes in an absorption system. *Int J Heat Mass Tran* 2019;**133**:1121–33.
[22] Libotean S, Salavera D, Valles M *et al.* Vapor-liquid equilibrium of ammonia plus lithium nitrate plus water and ammonia plus lithium nitrate solutions from (293.15 to 353.15) K. *J Chem Eng Data* 2007;**52**:1050–5.
[23] Libotean S, Martin A, Salavera D *et al.* Densities, viscosities, and heat capacities of ammonia plus lithium nitrate and ammonia plus lithium nitrate plus water solutions between (293.15 and 353.15) K. *J Chem Eng Data* 2008;**53**:2383–8.
[24] Chaudhari SK, Salavera D, Densities CA. Viscosities, heat capacities, and vapor-liquid equilibria of ammonia plus sodium thiocyanate solutions at several temperatures. *J Chem Eng Data* 2011;**56**:2861–9.
[25] Farshi LG, Ferreira CI, Mahmoudi S *et al.* Corrigendum to "first and second law analysis of ammonia/salt absorption refrigeration systems". *Int J Refrig* 2020;**109**:210–1.
[26] Ferreira CAI. Thermodynamic and physical property data equations for ammonia-lithium nitrate and ammonia-sodium thiocyanate solutions. *Sol Energy* 1984;**32**:231–6.
[27] Bakhtiari B, Fradette L, Legros R *et al.* A model for analysis and design of H_2O-LiBr absorption heat pumps. *Energ Convers Manage* 2011;**52**:1439–48.
[28] Li XT, Wu W, Zhang XL *et al.* Energy saving potential of low temperature hot water system based on air source absorption heat pump. *Appl Therm Eng* 2012;**48**:317–24.